Supporting Information

Machine Learning-Advanced Hydrogel-Based Transcription-Coupled Positive-Feedback CRISPR/Cas13a Analysis for Novel MicroRNA Signatures in Differential Diagnosis of Non-Small Cell Lung Cancer

Yi Zhang[1,2,†], Yuzhi Wang[3,†], Deyu Ma[2,†], Guangjun Xiao[4,†], Lin Feng[2], Jialiang Cai[2], Yuanjiu Xu[1], Yongjian Wang[1], Xiaoyu Liu[1], Jiangchuan Tian[1], Zhong Zuo[5,*], Jianhua Lan[6,*], Bo Shen[7,*], Shijia Ding[2,*]

[1]Department of Laboratory Medicine, West China Hospital, Sichuan University Sichuan University West China Hospital Guang'an Hospital, Guang'an People's Hospital, Guang'an, 638000, Sichuan, PR China

[2]Key Laboratory of Clinical Laboratory Diagnostics (Ministry of Education), College of Laboratory Medicine, Chongqing Medical University, Chongqing, 400016, PR China

[3]Department of Laboratory Medicine, Deyang People's Hospital, Deyang, 618000, Sichuan, PR China

[4]Department of Clinical Laboratory, Suining Central Hospital, Suining, 629000, PR China

[5]Department of Cardiology, The First Affiliated Hospital of Chongqing Medical University, Chongqing Medical University, Chongqing, 400016, PR China

[6]Department of Urology, West China Hospital, Sichuan University Sichuan University West China Hospital Guang'an Hospital, Guang'an People's Hospital, Guang'an, 638000, Sichuan, PR China

[7]Department of Laboratory Medicine, Chongqing Traditional Chinese Medicine Hospital, Chongqing, 400021, PR China

---

*Corresponding author.

E-mail address: dingshijia@163.com and dingshijia@cqmu.edu.cn (S. Ding); shenboszy228@163.com (B. Shen); ljhdoctor@yeah.net (J. Lan); zzuo-cq@hotmail.com (Z. Zuo).

[†]These authors contributed equally to this work.

Table of Contents

Figure S1. 1

Figure S2. 2

Figure S3. 3

Figure S4. 4

Figure S5. 5

Figure S6. 6

Figure S7. 7

Figure S8. 8

Figure S9. 9

Figure S10. 10

Figure S11. 11

Figure S12. 12

Figure S13. 13

Figure S14. 14

Table S1. 15

Table S2. 16

Table S3. 17

Table S4. 18

Table S5 19

Table S6. 20

Table S7. 21

Table S8. 22

Table S9. 25

Table S10. 28

Supplementary Methods 29

References 33

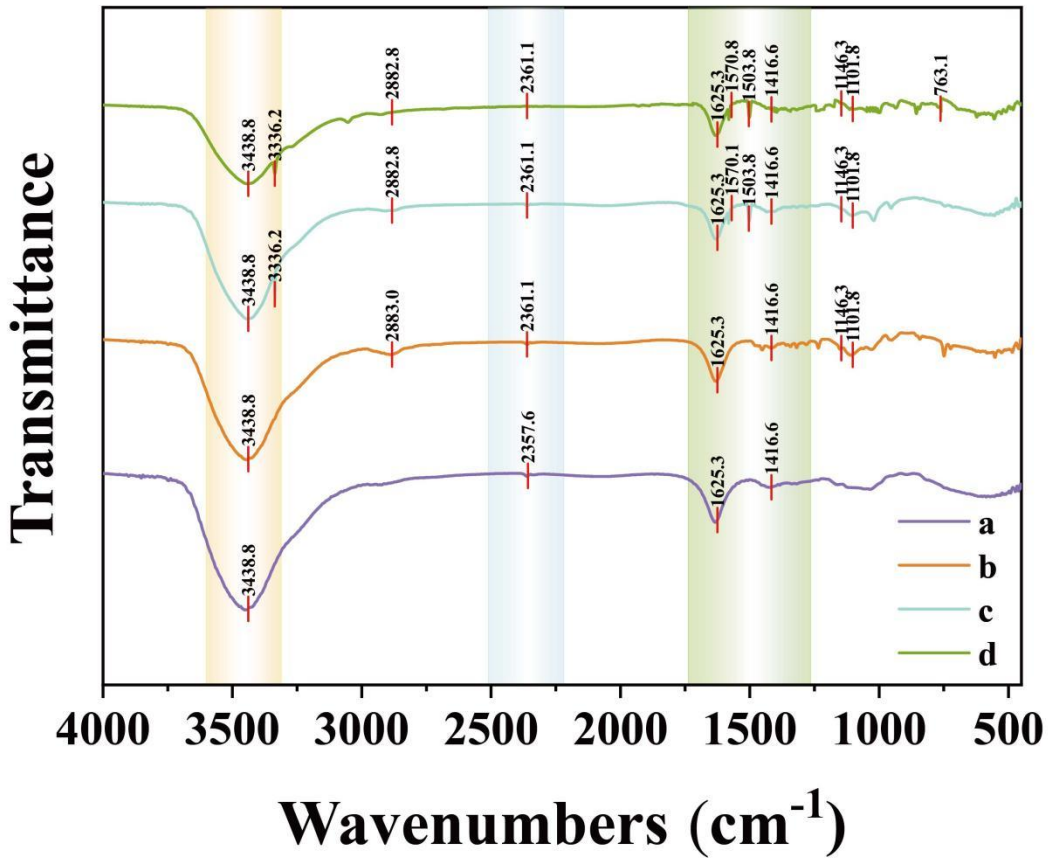


Figure S1. FT-IR spectra of (a) SA, (b) SA-PEG, (c) ACZ-SA-PEG, and (d) Au@ACZ-SA-PEG hydrogels.

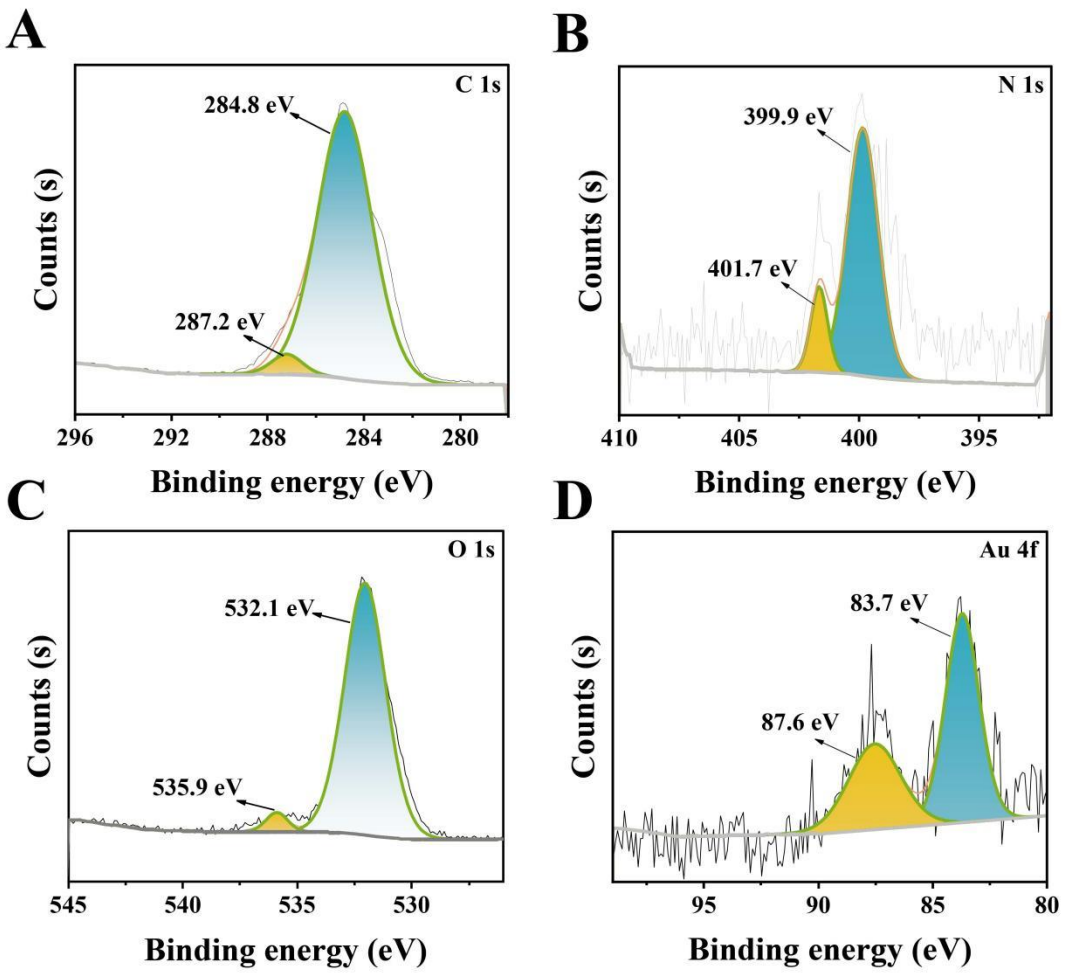


Figure S2. (A-D) High resolution XPS spectra of Au@ACZ-SA-PEG hydrogels for C 1s, N 1s, O 1s, and Au 4f.

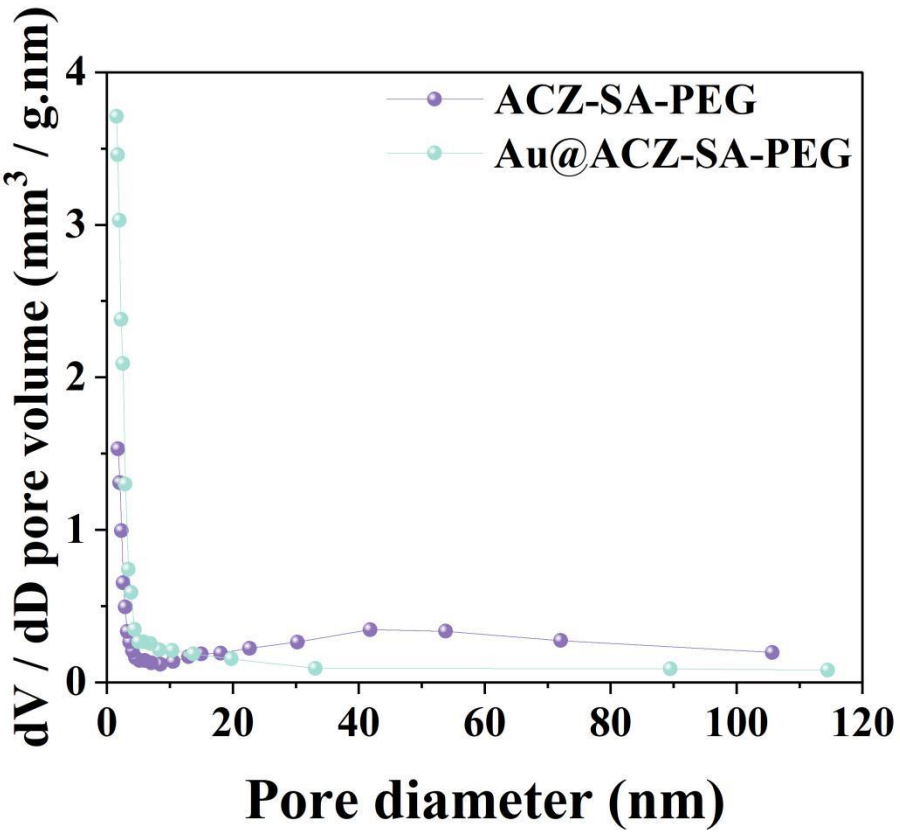


Figure S3. Pore-size distribution of ACZ-SA-PEG and Au@ACZ-SA-PEG hydrogels.

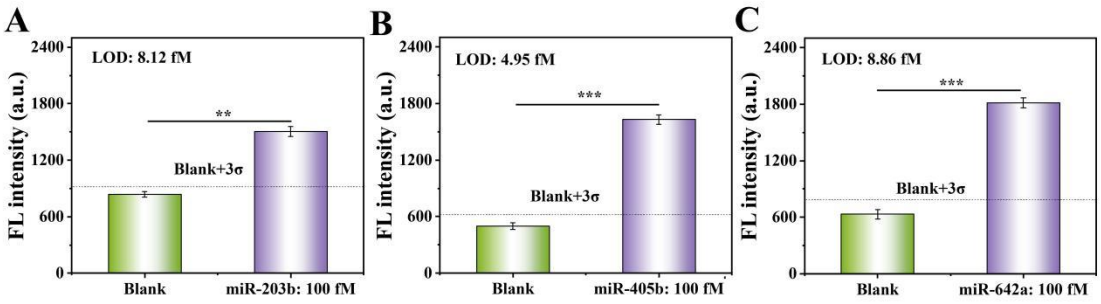


Figure S4. LODs of the TCPFC strategy for miR-203b, miR-450b, and miR-642a.

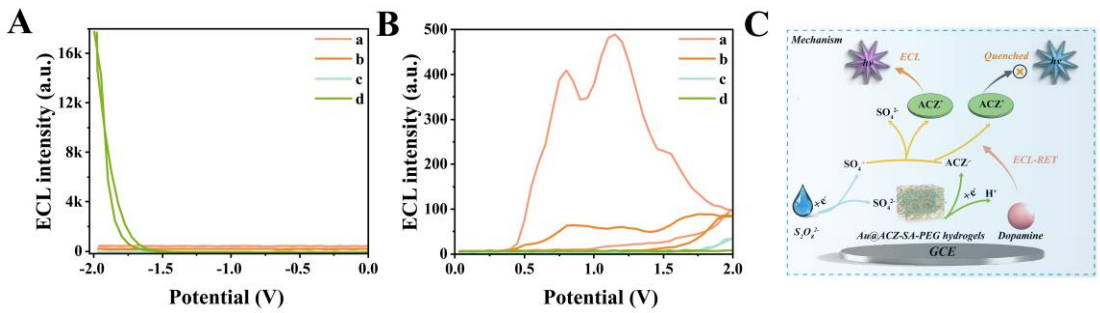


Figure S5. (A, B) ECL-potential obtained at the Au@ACZ-SA-PEG hydrogels/GCE with different co-reactants at negative electrode and positive electrode (a, 30 mM TEA; b, 30 mM TPA; c, 30 mM H_2O_2; d, 30 mM $K_2S_2O_8$). (C) Possible ECL luminescence mechanism of Au@ACZ-SA-PEG hydrogels.

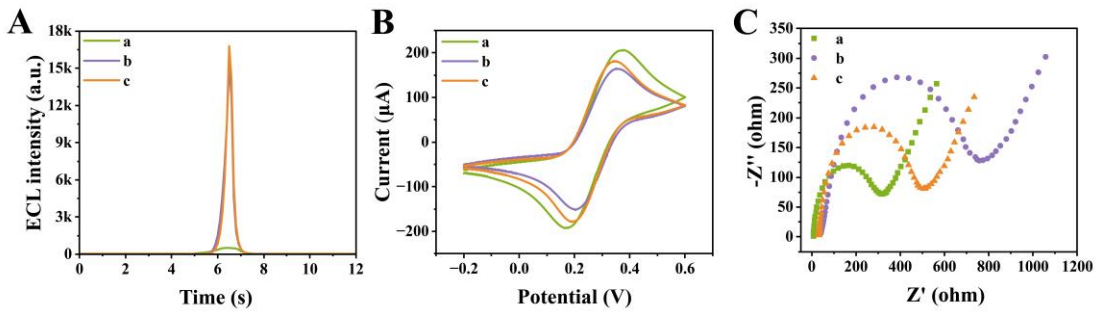


Figure S6. (A) ECL intensity, (B) CV, and (C) EIS plots of (a) SA-PEG, (b) ACZ-SA-PEG and (c) Au@ACZ-SA-PEG.

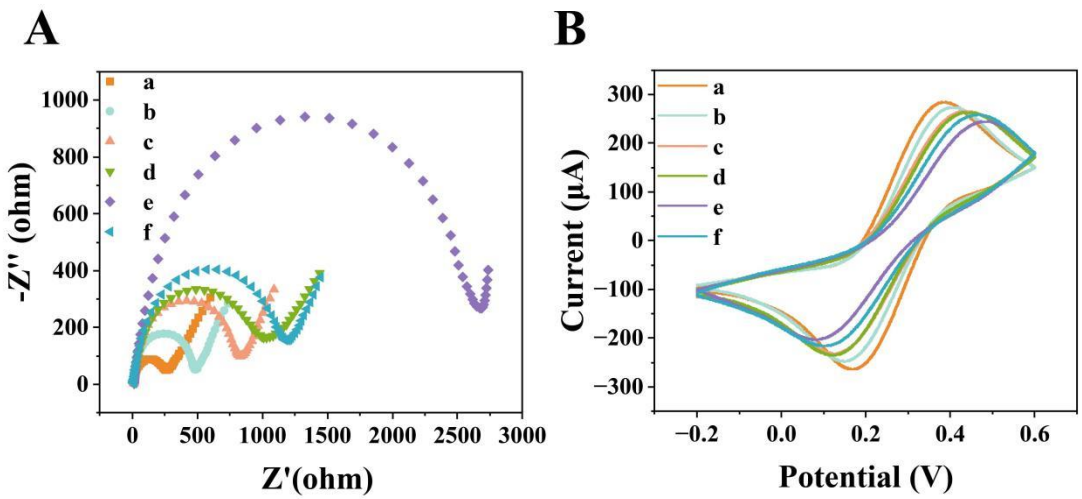


Figure S7. (A) EIS plots and (B) CV curves of (a) bare GCE, (b) GCE/Au@ACZ-SA-PEG hydrogels, (c) GCE/Au@ACZ-SA-PEG hydrogels/S1, (d) GCE/Au@ACZ-SA-PEG hydrogels/S1/MCH, (e) GCE/Au@ACZ-SA-PEG hydrogels/S1/MCH/S2-DA, and (f) after addition into the TCPFC strategy.

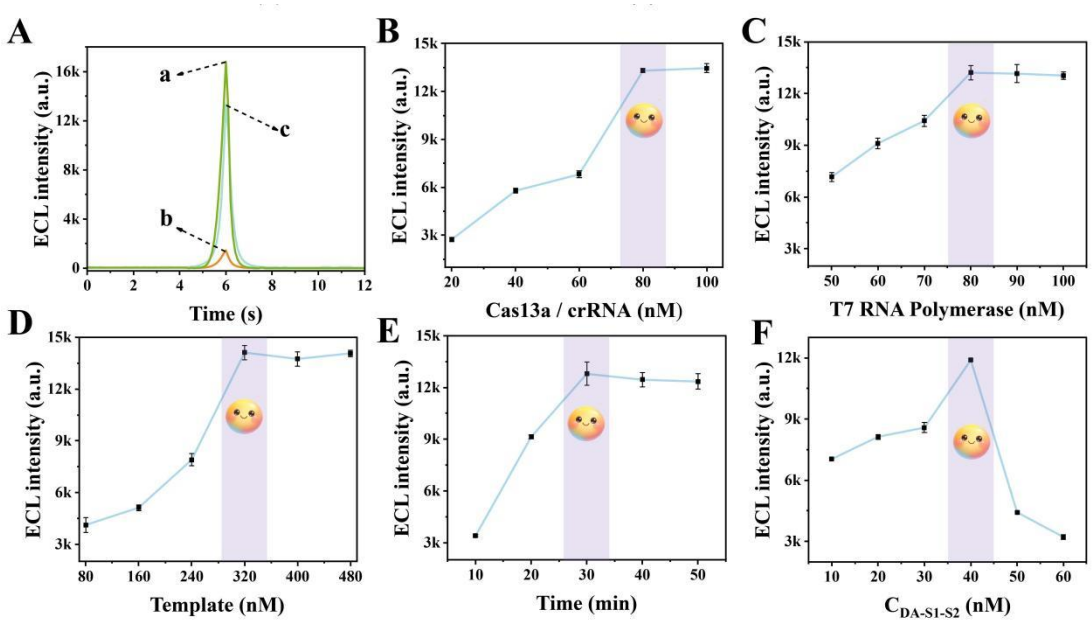


Figure S8. (A) DA-driven ECL signal switching biosensor. (B-D) Optimization of the experimental conditions (The concentration of Cas13a/crRNA, T7 RNA polymerase, and template). (E) Optimization of incubation time of the TCPFC strategy. (F) Optimization of S1-S2-DA concentration. Emoji symbols used in each figure denote the optimal experimental conditions selected for subsequent experiments.

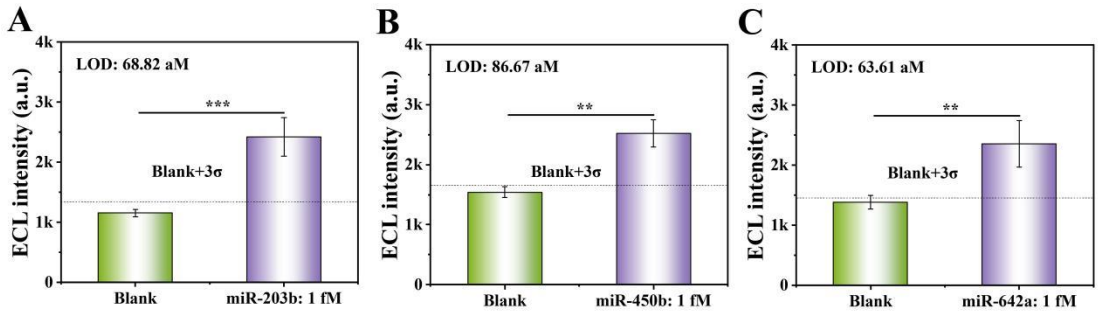


Figure S9. LODs of the ECL biosensor for miR-203b, miR-450b and miR-642a.

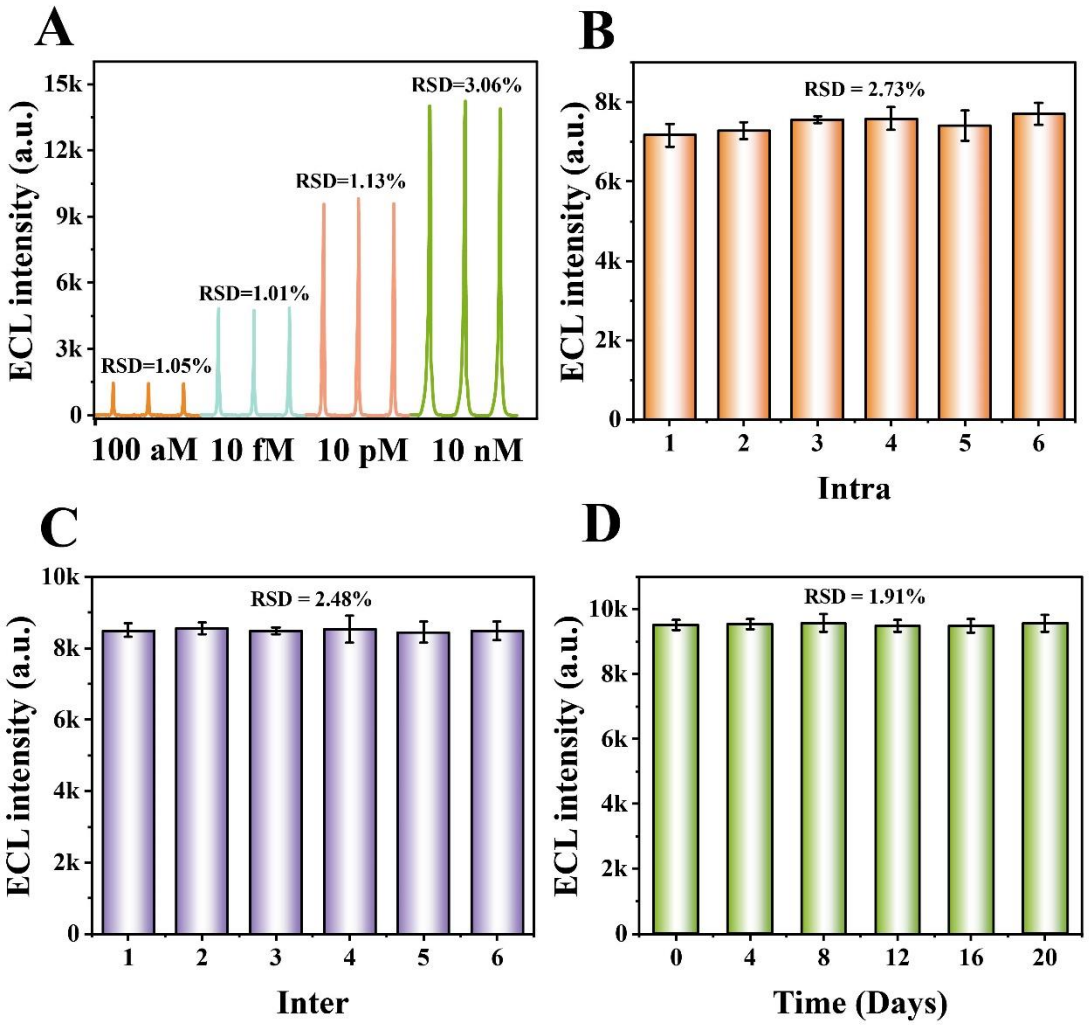


Figure S10. (A) Stability of the ECL assay for miR-203b. (B, C) Reproducibility of the biosensor in six parallel intra-assays and inter-assays with 10 pM miR-203b. (D) Storage stability of 10 pM miR-203b for 20 days of the ECL biosensor.

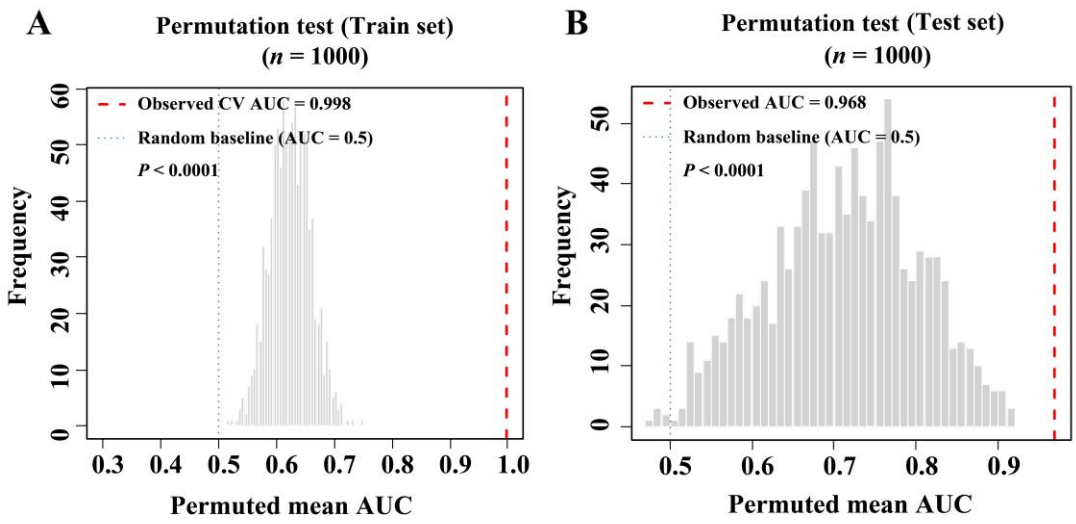


Figure S11. Permutation test results for the GBM model in the train and test sets.

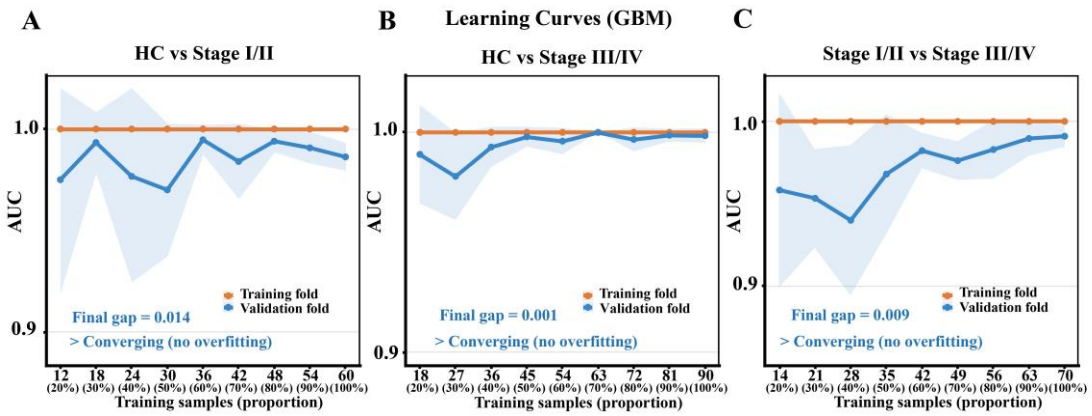


Figure S12. Learning curves for the GBM model across three pairwise comparisons in the train set.

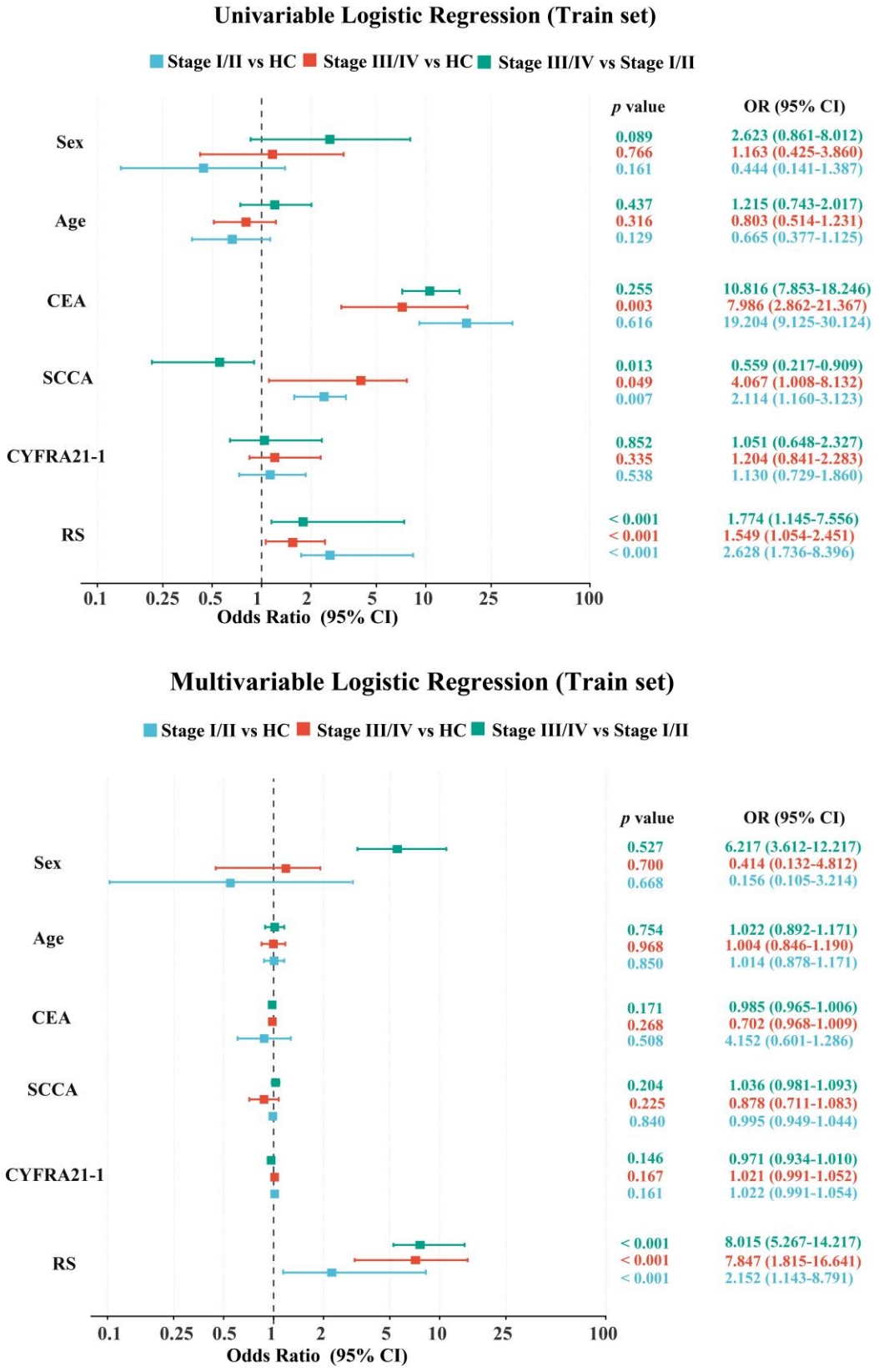


Figure S13. Forest plot of univariate and multivariate logistic regression analysis in the train set.

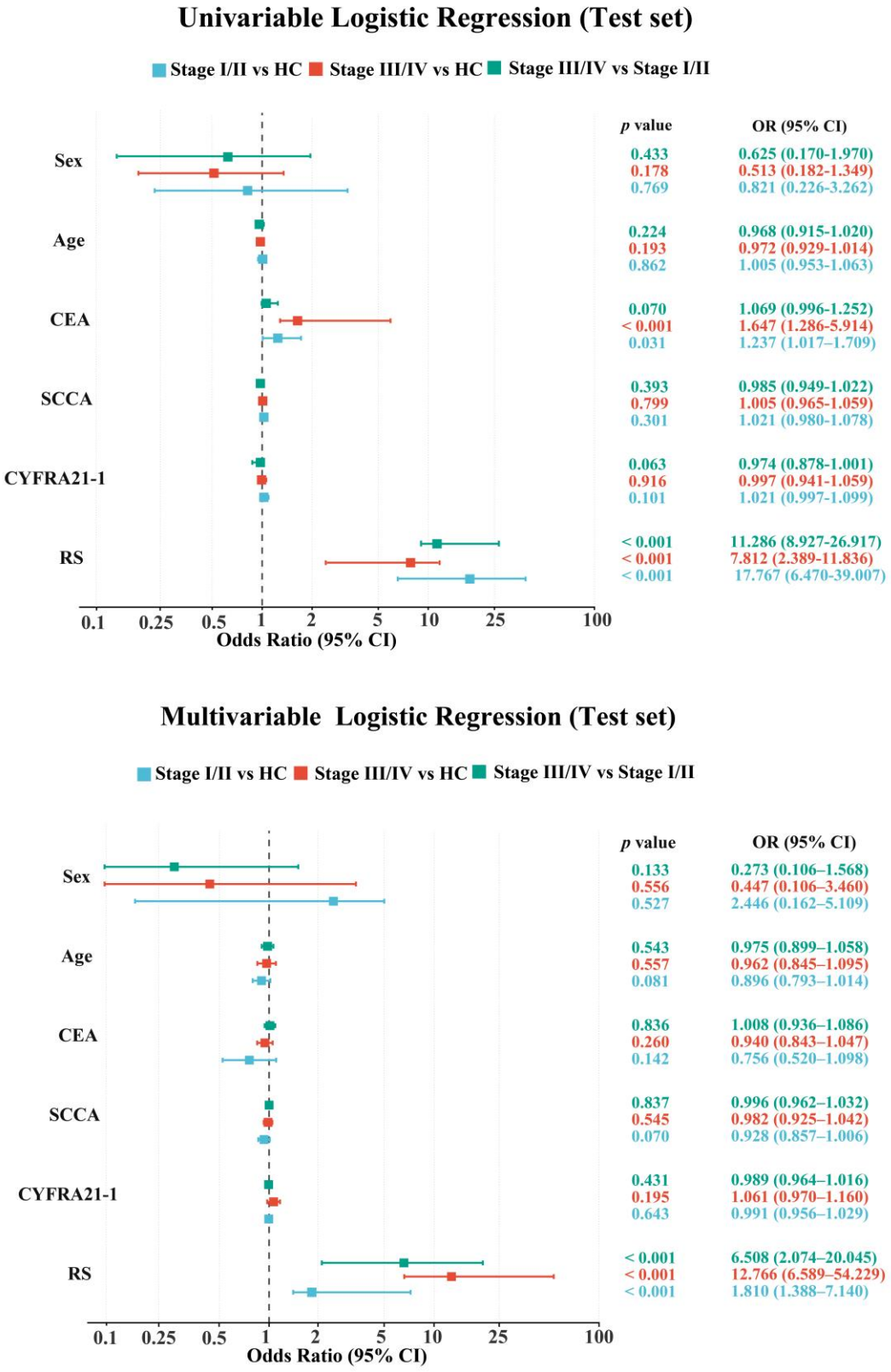


Figure S14. Forest plot of univariate and multivariate logistic regression analysis in the test set.

Table S1. The nucleic acid sequences employed in the present work.

miRNA	Name	Sequence (5'-3')
miR-450b	crRNA	GAUUUAGACUACCCCAAAAACGAAGGGGACUAAAACUA UUCAGGAACAUAUUGCAAAA
	Template	TAATACGACTCAUUTUUTATTCAGGAACATATTGCAAAAC CCTATAGTGAGTCGTATTA
miR-203b	crRNA	GAUUUAGACUACCCCAAAAACGAAGGGGACUAAAACUG UGAAAUGUUUAGGACCACUA
	Template	TAATACGACTCAUUTUUTGTGAAATGTTTAGGACCACTAC CCTATAGTGAGTCGTATTA
miR-642a	crRNA	GAUUUAGACUACCCCAAAAACGAAGGGGACUAAAACCAA GACACAUUUGGAGAGGGAC
	Template	TAATACGACTCAUUTUUCAAGACACATTTGGAGAGGGACC CCTATAGTGAGTCGTATTA
	ssRNA	FAM-CCCCCAUUUUUACCTCAUUUUUTTGATGGGGG-BHQ1
	S1	HS-SH C6-TTTTTTTTTTCGTACGTAATAGCTGCA
	S2	COOH-TTTUUUUUTGCAGCTATTACGTACG

Table S2. Sequences of target and primer in PCR.

Name	Sequence (5'-3')
miR-566	GGGCGCCUGUGAUCCCAAC
miR-566-F	GGCGCCTGTGATCCCAAC
miR-218	UUGUGCUUGAUCUAACCAUGU
miR-218-F	GCCGTTGTGCTTGATCTAACCATGT
miR-450b	UUUUGCAAUAUGUUCCUGAAUA
miR-450b-F	GCCGCTTTTGCAATATGTTCCTGAATA
miR-661	UGCCUGGGUCUCUGGCCUGCGCGU
miR-661-F	CTGGGTCTCTGGCCTGC
miR-203b	UAGUGGUCCUAAACAUUUCACA
miR-203b-F	GCCTAGTGGTCCTAAACATTTCACA
miR-642a	GUCCCUCUCCAAAUGUGUCUUG
miR-642a-F	GGTCCCTCTCCAAATGTGTCTTG
miR-193a	UGGGUCUUUGCGGGCGAGAUGA
miR-193a-F	CTCTTTGCGGGCGAGATGA
miR-345	GCUGACUCCUAGUCCAGGGCUC
miR-345-F	GCTGACTCCTAGTCCAGGG

F: forward primer

Table S3. PCR reaction system.

Reagents	50 μL reaction system	Final concentration
2 x miRcute Plus miRNA premix	25 μL	1 x
Forward primer (10 μM)	1 μL	200 nM
Reverse primer (10 μM)	1 μL	200 nM
Template cDNA	2 μL	
RNase-free-ddH_2O	21 μL	

Table S4. PCR procedure.

Program	Temperature/℃	Duration/s
Preincubation	95	900
2 step amplification	94	20
(40 cycles)	60	34
Melting analysis	95	10
	65	60
	97	1

Table S5. Comparison with different biosensors for miRNA detection.

Detection methods	Linear range	LOD	Ref.
Fluorescence	50 fM ~10 nM	20.42 fM	[1]
Electrochemiluminescence	1 fM ~ 1 nM	273.20 aM	[2]
Fluorescence	10 fM ~ 10 nM	2.10 and 4.40 fM	[3]
Electrochemiluminescence	100 aM ~ 10 nM	100.00 aM	[4]
Electrochemistry	2 fM ~ 200 nM	150.00 aM	[5]
Electrochemiluminescence	1 fM ~ 500 pM	0.45 fM	[6]
Electrochemiluminescence	10 fM ~ 10 nM	2.44 fM	[7]
Electrochemiluminescence	**100 aM ~ 1 nM**	**68.82, 86.67, and 63.61 aM**	**This work**

Table S6. Analytical application of the biosensor in diluted human plasma samples.

Sample	Addition (pM)	ECL intensity (a.u.)	Found (pM)	RSD (%, *n*=3)	Recovery (%, *n*=3)
1	0.01	5253	0.01	2.14	107.11%
2	1.00	8796	1.03	1.36	103.23%
3	100.00	12362	102.20	0.98	102.49%

.

Table S7. A comparison of the cost and assay time among RT-qPCR and this work.

Comparison types	RT-qPCR	This work
Reagents cost ($)	5.92	5.75
Assay time (minutes)	87.64	33.34

Table S8. Clinical sample information of train cohort.

Number	Sex	Age	Group	CEA	SCCA	CYFRA21-1
H1	Male	58	HC	5.57	1.11	3.96
H2	Female	80	HC	2.28	0.84	2.77
H3	Male	59	HC	5.42	1.62	1.94
H4	Male	69	HC	3.16	0.35	3.05
H5	Female	62	HC	3.24	0.12	1.2
H6	Male	57	HC	5.03	0.28	1.76
H7	Male	71	HC	2.79	0.38	3.96
H8	Male	71	HC	0.93	0.62	3.38
H9	Male	72	HC	1.89	1.69	3.38
H10	Male	72	HC	3.70	1.57	1.87
H11	Male	57	HC	2.55	0.16	1.32
H12	Male	51	HC	0.54	1.16	1.03
H13	Female	55	HC	1.85	0.04	2.09
H14	Female	62	HC	5.80	0.50	0.18
H15	Male	62	HC	3.28	1.57	2.84
H16	Male	75	HC	4.00	0.40	3.35
H17	Male	68	HC	5.46	0.90	3.12
H18	Male	50	HC	3.22	0.65	3.08
H19	Male	72	HC	1.83	1.18	2.92
H20	Male	75	HC	3.75	0.37	2.15
H21	Male	66	HC	0.08	0.73	3.09
H22	Male	67	HC	3.52	0.56	3.51
H23	Female	59	HC	5.32	1.70	2.77
H24	Female	70	HC	0.04	0.14	2.02
H25	Male	72	HC	5.13	0.20	0.88
H26	Male	71	HC	4.04	1.31	2.37
H27	Male	62	HC	3.38	1.53	1.25
H28	Male	55	HC	2.91	1.04	3.5
H29	Male	66	HC	5.85	0.38	2.37
H30	Female	82	HC	5.80	0.46	1.35
H31	Male	72	HC	1.17	1.39	2.80
H32	Male	64	HC	5.03	0.73	2.90
H33	Male	63	HC	3.53	0.54	1.55
H34	Male	69	HC	2.35	1.23	3.35
H35	Female	69	HC	4.28	1.62	1.36
H36	Male	63	HC	1.07	1.26	2.93
H37	Male	73	HC	3.59	0.73	0.97
H38	Female	68	HC	2.38	1.00	6.40
H39	Male	67	HC	1.07	1.00	6.69
H40	Male	62	HC	1.07	0.84	20.22

P1	Male	68	Stage I/II	2.04	44.70	1.20
P2	Male	71	Stage I/II	2.09	2.90	6.30
P3	Male	60	Stage I/II	1.92	84.20	8.83
P4	Male	73	Stage I/II	1.99	21.60	1.70
P5	Male	68	Stage I/II	12.26	0.60	21.48
P6	Female	79	Stage I/II	1.49	0.70	1.70
P7	Male	51	Stage I/II	8.83	0.60	6.98
P8	Male	65	Stage I/II	0.88	0.70	3.36
P9	Female	70	Stage I/II	1.66	5.80	6.30
P10	Male	69	Stage I/II	0.57	1.40	27.80
P11	Male	73	Stage I/II	2.53	0.60	6.40
P12	Male	54	Stage I/II	6.29	0.50	2.95
P13	Male	44	Stage I/II	1.39	4.30	1.80
P14	Female	59	Stage I/II	2.24	44.7	26.97
P15	Female	49	Stage I/II	0.77	0.90	24.5
P16	Male	63	Stage I/II	0.93	0.70	2.10
P17	Female	53	Stage I/II	0.89	0.60	3.42
P18	Female	60	Stage I/II	4.18	0.70	12.24
P19	Female	62	Stage I/II	0.79	0.60	4.40
P20	Female	60	Stage I/II	1.33	0.60	1.10
P21	Male	74	Stage III/IV	69.89	0.90	2.00
P22	Male	62	Stage III/IV	0.78	2.80	3.50
P23	Male	63	Stage III/IV	3.27	1.80	9.80
P24	Male	75	Stage III/IV	5.07	2.50	21.62
P25	Male	58	Stage III/IV	2.72	0.80	6.70
P26	Male	69	Stage III/IV	31.07	1.10	33.10
P27	Male	68	Stage III/IV	5.63	6.20	9.80
P28	Male	62	Stage III/IV	1.82	0.70	3.30
P29	Male	59	Stage III/IV	5.24	0.70	1.46
P30	Female	48	Stage III/IV	1.08	0.50	4.80
P31	Female	76	Stage III/IV	2.35	0.60	16.72
P32	Male	62	Stage III/IV	4.21	2.00	8.35
P33	Male	61	Stage III/IV	23.16	1.20	2.50
P34	Male	69	Stage III/IV	2.98	15.20	1.00
P35	Male	54	Stage III/IV	5.93	1.40	2.92
P36	Female	59	Stage III/IV	6.19	0.60	2.59
P37	Male	68	Stage III/IV	6.59	7.90	6.40
P38	Male	62	Stage III/IV	4.12	0.70	15.8
P39	Female	56	Stage III/IV	5.04	0.70	9.37
P40	Male	73	Stage III/IV	1.17	1.00	3.72
P41	Male	58	Stage III/IV	15.32	0.80	4.00
P42	Male	65	Stage III/IV	4.32	0.50	6.69
P43	Female	68	Stage III/IV	23.27	0.40	28.50

P44	Female	63	Stage III/IV	2.92	2.20	2.10
P45	Male	58	Stage III/IV	10.89	0.70	1.30
P46	Male	54	Stage III/IV	3.56	20.4	4.23
P47	Male	67	Stage III/IV	4.88	0.90	2.10
P48	Male	75	Stage III/IV	1.50	0.60	6.40
P49	Female	73	Stage III/IV	5.09	0.90	48.06
P50	Male	61	Stage III/IV	1.20	0.90	2.15
P51	Male	72	Stage III/IV	2.44	0.50	48.5
P52	Male	63	Stage III/IV	1.07	0.60	12.67
P53	Male	72	Stage III/IV	2.99	0.30	2.49
P54	Male	61	Stage III/IV	18.41	0.70	3.60
P55	Male	68	Stage III/IV	1.51	1.00	3.08
P56	Male	73	Stage III/IV	3.42	0.50	1.90
P57	Female	43	Stage III/IV	4.18	3.30	7.36
P58	Male	70	Stage III/IV	1.46	0.70	6.90
P59	Female	54	Stage III/IV	23.01	0.80	2.40
P60	Male	74	Stage III/IV	213.97	0.30	2.11
P61	Male	79	Stage III/IV	6.07	0.02	113.80
P62	Male	58	Stage III/IV	169.15	1.25	1.40
P63	Male	58	Stage III/IV	2.99	0.81	1.80
P64	Female	62	Stage III/IV	2.62	1.16	5.80
P65	Male	68	Stage III/IV	12.01	1.40	20.22
P66	Male	57	Stage III/IV	3.77	1.64	3.74
P67	Male	60	Stage III/IV	1.14	0.09	5.30
P68	Male	59	Stage III/IV	1.53	1.45	4.90
P69	Male	60	Stage III/IV	4.94	1.17	2.80
P70	Male	83	Stage III/IV	11.46	1.67	3.00

Table S9. Clinical sample information of test cohort.

Number	Sex	Age	Group	CEA	SCCA	CYFRA21-1
H1	Male	72	HC	4.14	0.97	3.15
H2	Female	73	HC	4.54	1.27	1.39
H3	Male	71	HC	1.97	0.21	3.34
H4	Male	76	HC	0.50	0.75	1.79
H5	Male	69	HC	1.60	0.69	3.26
H6	Male	74	HC	2.51	1.54	0.35
H7	Female	37	HC	0.06	1.39	2.15
H8	Male	59	HC	5.18	0.28	1.66
H9	Female	74	HC	4.55	0.66	3.77
H10	Male	55	HC	0.34	0.56	3.59
H11	Male	77	HC	3.52	0.16	1.21
H12	Male	67	HC	3.45	0.90	0.82
H13	Male	57	HC	5.66	1.66	0.28
H14	Male	62	HC	2.09	0.24	0.65
H15	Male	62	HC	1.11	1.03	0.71
H16	Male	61	HC	1.46	0.74	2.60
H17	Male	85	HC	5.32	1.17	3.03
H18	Male	56	HC	3.95	0.05	0.65
H19	Female	52	HC	3.49	1.53	2.96
H20	Male	60	HC	1.74	0.27	2.76
H21	Male	68	HC	2.88	1.08	1.23
H22	Male	58	HC	2.19	0.50	3.45
H23	Male	67	HC	4.79	1.79	2.29
H24	Male	62	HC	1.17	0.81	4.23
H25	Male	73	HC	0.54	0.90	2.50
H26	Male	76	HC	0.54	0.90	2.80
H27	Male	68	HC	4.28	44.70	1.46
H28	Male	67	HC	2.38	0.60	1.46
H29	Male	75	HC	4.28	3.30	48.5
H30	Female	73	HC	2.38	4.30	3.24
H31	Male	61	HC	0.54	1.70	3.24
H32	Male	72	HC	2.91	2.20	4.42
H33	Male	63	HC	1.92	0.50	2.80
H34	Male	72	HC	2.91	1.70	7.36
H35	Male	61	HC	0.04	0.81	1.82
H36	Male	68	HC	0.54	0.84	1.82
H37	Male	73	HC	2.91	0.7	20.22
H38	Female	43	HC	1.17	0.97	6.40
H39	Male	70	HC	1.07	1.00	6.69
H40	Female	54	HC	0.54	0.97	6.40
P1	Male	74	Stage I/II	9.33	1.30	3.46

P2	Male	79	Stage I/II	2.53	2.10	31.50
P3	Male	58	Stage III/IV	2.95	1.50	2.93
P4	Male	58	Stage III/IV	5.00	3.30	2.10
P5	Female	62	Stage III/IV	3.26	0.60	23.70
P6	Male	68	Stage III/IV	0.50	3.30	32.90
P7	Male	57	Stage III/IV	12.43	10.90	1.48
P8	Male	60	Stage III/IV	19.12	2.90	1.70
P9	Male	59	Stage I/II	2.88	1.30	5.72
P10	Male	60	Stage III/IV	2.25	0.30	12.80
P11	Male	83	Stage III/IV	1.96	0.50	2.18
P12	Male	72	Stage III/IV	2.58	0.30	8.80
P13	Female	73	Stage III/IV	3.05	1.30	3.40
P14	Male	71	Stage III/IV	1.94	0.50	3.15
P15	Male	76	Stage III/IV	4.51	70.00	2.10
P16	Male	69	Stage III/IV	2.96	0.80	2.46
P17	Male	74	Stage III/IV	1.60	0.70	11.59
P18	Female	37	Stage III/IV	2.77	1.70	1.71
P19	Male	59	Stage III/IV	2.38	1.80	145.1
P20	Female	74	Stage III/IV	2.87	0.60	2.11
P21	Male	55	Stage III/IV	7.35	0.80	13.7
P22	Male	77	Stage III/IV	2.16	3.70	5.03
P23	Male	67	Stage III/IV	4.69	0.60	33.75
P24	Male	57	Stage III/IV	17.44	1.70	2.40
P25	Male	62	Stage III/IV	2.05	3.60	2.30
P26	Male	62	Stage III/IV	2.66	3.40	6.10
P27	Male	61	Stage III/IV	30.05	7.30	9.00
P28	Male	85	Stage III/IV	3.27	0.80	1.33
P29	Male	56	Stage I/II	1.37	0.80	4.80
P30	Female	52	Stage I/II	41.37	1.60	1.82
P31	Male	60	Stage I/II	4.47	0.60	1.86
P32	Male	68	Stage I/II	6.30	1.70	3.94
P33	Male	58	Stage I/II	5.19	0.70	3.46
P34	Male	67	Stage I/II	5.01	1.00	1.80
P35	Male	62	Stage I/II	1.89	2.00	1.90
P36	Male	73	Stage I/II	4.65	1.00	0.64
P37	Male	76	Stage I/II	7.26	0.60	10.00
P38	Male	68	Stage I/II	2.65	2.80	1.50
P39	Female	60	Stage I/II	42.53	1.20	1.37
P40	Male	40	Stage I/II	2.61	0.40	5.54
P41	Female	52	Stage I/II	9.04	2.10	0.58
P42	Female	54	Stage I/II	6.15	0.80	0.31
P43	Male	68	Stage I/II	2.62	0.60	1.29
P44	Male	55	Stage I/II	6.21	0.40	7.08

P45	Female	51	Stage I/II	12.97	0.50	11.30
P46	Male	57	Stage III/IV	0.54	1.70	2.70
P47	Male	61	Stage III/IV	2.96	0.70	4.05
P48	Male	72	Stage III/IV	3.38	0.90	6.94
P49	Female	71	Stage III/IV	1.68	0.90	5.89
P50	Male	56	Stage III/IV	1.52	0.80	2.94
P51	Male	77	Stage III/IV	5.25	0.60	0.60
P52	Female	74	Stage III/IV	22.02	1.50	1.30
P53	Male	66	Stage III/IV	13.47	0.60	2.50
P54	Female	70	Stage III/IV	3.69	10.10	3.24
P55	Female	60	Stage III/IV	9.47	3.30	4.42
P56	Female	44	Stage III/IV	4.57	0.70	17.7
P57	Male	65	Stage III/IV	6.74	0.50	3.94
P58	Female	74	Stage III/IV	6.69	70.00	1.81
P59	Male	65	Stage III/IV	6.13	2.00	5.56
P60	Female	70	Stage III/IV	58.79	1.23	4.24
P61	Male	76	Stage III/IV	1.05	0.39	1.69
P62	Female	70	Stage III/IV	7.60	0.41	5.06
P63	Female	47	Stage III/IV	3.77	1.31	6.99
P64	Female	51	Stage III/IV	5.30	0.72	7.51
P65	Male	68	Stage III/IV	8.22	0.39	0.65
P66	Male	59	Stage III/IV	19.12	1.10	2.42
P67	Male	49	Stage III/IV	5.14	0.99	3.64
P68	Male	55	Stage III/IV	3.47	0.52	6.40
P69	Male	80	Stage III/IV	3.99	0.75	2.59
P70	Male	60	Stage III/IV	48.47	1.06	2.00

Table S10. Hyperparameter optimization summary for all 16 machine learning algorithms.

Algorithms	Hyperparameters tuned	Search strategy	Selection criterion
LASSO	λ (100 log-spaced values)	cv.glmnet, 5-fold CV	Min. classification error
Ridge	λ (100 log-spaced values)	cv.glmnet, 5-fold CV	Min. classification error
Elastic Net	λ (100 values; α fixed = 0.5)	cv.glmnet, 5-fold CV	Min. classification error
Stepglm	Weight decay (5 candidates)	caret, 5-fold CV	Max. mean AUC
SVM	C (0.25–8); σ (0.0625–0.5) (24 pairs)	Grid search, 5-fold CV	Max. mean AUC
RF	mtry (1, 2, …, [√p])	Grid search, 5-fold CV	Max. mean AUC
GBM	n.trees (up to 3,000)	5-fold internal CV	Min. log-loss
XGBoost	nrounds (up to 500)	5-fold CV + early stopping (20 rds)	Min. log-loss
glmBoost	mstop, prune (5 candidates each)	caret, 5-fold CV	Max. mean AUC
plsRglm	nt - no. of components (5 candidates)	caret, 5-fold CV	Max. mean AUC
SDA	λ, δ (5 candidates each)	caret, 5-fold CV	Max. mean AUC
RDA	λ, γ (5 candidates each)	caret, 5-fold CV	Max. mean AUC
CART	cp - complexity parameter (5 candidates)	caret, 5-fold CV	Max. mean AUC
LDA	None (closed-form solution)	NA	NA
Naive Bayes	None (Gaussian assumption)	NA	NA

AUC, area under the receiver operating characteristic curve; CV, cross-validation; rds, rounds; p, number of input features. NA denotes not applicable.

Supplementary Methods

Material and Reagents

Sodium alginate (SA), polyethylene glycol (PEG), potassium persulfate ($K_2S_2O_8$), N-hydroxysuccinimide (NHS), N-(3-dimethylaminopropyl)-N-ethylcarbodiimide hydrochloride (EDC), and dopamine (DA) were obtained from Sigma-Aldrich Co., Ltd. (St. Louis, MO, USA). Chloroauric acid hexahydrate ($HAuCl_4 \cdot 6H_2O$) and calcium chloride ($CaCl_2$) were purchased from Aladdin (Shanghai, China), while 9H-Carbazol-9-amine (ACZ) and MES hydrate ($C_6H_{13}NO_4S \cdot H_2O$) were acquired from Macklin Inc. (Shanghai, China). LIXI BIOLOGY Inc (5 μM stock, Catalog No. LXC007M, LIXI Biology, Wuhan, China) supplied the LwaCas13a. All nucleic acid strands (Table S1), RNase inhibitor, and NTP mixture solutions were purchased from Sangon Biotechnology Co. Ltd. (Shanghai, China). The total RNA extraction kit and RT-qPCR two-step kit were purchased from Tiangen Biotech (Beijing, China). The oligonucleotides were dissolved in TE buffer (10 mM Tris-HCl, 1 mM ethylenediaminetetraacetic acid (EDTA), pH 8.0), and stored at -20 °C. The buffers used in this study were prepared as follows: 0.1 M PBS buffer (1370 mM NaCl, 27 mM KCl, 100 mM Na_2HPO_4, 18 mM KH_2PO_4, pH 7.4). Sodium borohydride ($NaBH_4$), 6-mercapto-1-hexanol (MCH) and other reagents were purchased from Chemical Reagent Co., Ltd. (Chongqing, China). Deionized water employed in the experiment was prepared by Millipore water purification system (≥ 18.2 MΩ, Milli-Q, Millipore).

Apparatus

The electrochemiluminescence (ECL), cyclic voltammetry (CV), and electrochemical impedance spectroscopy (EIS) measurements were performed on the MPI-E multifunctional analyzer (Xi'an Remax Electronic Science &Technology Co., Ltd, China) and CHI660D electrochemistry workstation (Shanghai Chenhua Instruments Co., Ltd, Shanghai, China) with a conventional three-electrode system, respectively. The three-electrode system was composed of a platinum wire (counter electrode), an Ag/AgCl electrode (reference electrode), and a modified glassy carbon electrode (working electrode). Fluorescence signals were collected by the Agilent Eclipse Fluorescence Spectrophotometer (Agilent, USA). A thermal cycler (Thermo Fisher

Scientific, USA) was used for the PCR reactions. The morphologies of different materials were characterized using X-max energy dispersive spectroscopy (EDS, Berlin, Germany) and scanning electron microscopy (SEM, Hitachi, Japan), respectively. X-ray photoelectron spectra (XPS) were monitored with a Thermo ESCALAB 250Xi (USA). X-ray diffraction (XRD) patterns of the synthetic samples were obtained with a D8 ADVANCE X-ray diffractometer (Bruker, Germany) to confirm the structure of the materials. Atomic force microscopy (AFM) was conducted in tapping mode under ambient conditions using a commercial AFM (Bruker, USA) to characterize surface topography and quantify the root-mean-square roughness (Rq). Nitrogen gas adsorption pore size, pore volume, and Brunauer-Emmett-Teller (BET) specific surface area were determined using nitrogen gas adsorption in Micromeritics ASAP 2460 (Micromeritics, USA). The UV-vis absorption spectrum and Fourier Transform Infrared Spectroscopy (FT-IR) analysis were measured by a UV-2550 UV-vis spectrophotometer (Shimadzu, Tokyo, Japan) and Nicolet iS10 Fourier Transform Infrared spectrometer (Thermo Fisher Scientific, USA), respectively.

Extraction of cell free miRNAs in plasma

miRNA from plasma was isolated with the MiRcute miRNA Isolation Kit (TIANGEN Biotech, Beijing, China) and purified following the manufacturer's protocol. The extracted miRNA was quantified and assessed for purity with a NanoDrop spectrophotometer (Thermo Fisher Scientific, USA), stored at -80 °C until analysis.

RT-qPCR assay of miRNAs

First, 20 ng of extracted miRNA was reverse transcribed to cDNA with the miRNA First Strand cDNA Synthesis Kit (TIANGEN Biotech, China), which provided the Universal PCR Primer R as the reverse primer. Forward primer sequences are listed in Table S2 and were synthesized by Sangon Biotech. Primers and cDNA template were combined with miRcute Plus miRNA qPCR Kit (TIANGEN Biotech, China) according to the reaction composition in Table S3. Thermal cycling conditions followed Table S4 and reactions were run on a LightCycler 96 instrument (Thermo Fisher Scientific, USA).

Machine Learning Modeling

All 16 machine learning algorithms were trained with systematic hyperparameter

optimization performed exclusively within the train set using cross-validation; the test set was locked throughout and accessed only once for final evaluation. Linear discriminant analysis (LDA) and Naive Bayes, both of which require no hyperparameter optimization, were fitted directly on the full train set using the MASS and e1071 packages, respectively. LDA was implemented via its closed-form solution, and naive bayes via a Gaussian kernel with analytically estimated parameters.

For regularized regression, LASSO ($\alpha = 1$), Ridge ($\alpha = 0$), and Elastic Net ($\alpha = 0.5$) were implemented via the *"glmnet"* package with a grouped multinomial penalty. The regularization parameter λ was selected from 100 log-spaced candidates using 5-fold cross-validation minimizing multinomial classification error (λ_{min} criterion). Stepwise generalized linear model (Stepglm; forward, backward, and bidirectional) was implemented via the *"nnet"* package within *caret*, with the weight-decay parameter tuned over five log-spaced candidates (tuneLength = 5) by 5-fold cross-validation maximizing mean AUC; AIC-based variable selection was applied internally at each decay value.

Support vector machine (SVM; radial basis function kernel, one-versus-one strategy) was implemented via kernlab within caret. Two hyperparameters were jointly optimized by grid search with 5-fold cross-validation: the cost parameter C (0.25, 0.5, 1, 2, 4, 8) and the kernel bandwidth σ (0.0625, 0.125, 0.25, 0.5) (24 combinations; criterion: max. mean AUC). Random forest (RF) was built with 500 trees via the *"randomForest"* package within *caret*; the number of features sampled at each node split was tuned by grid search over (1, 2, …, $\lfloor\sqrt{p}\rfloor$) with 5-fold cross-validation maximizing mean AUC, with minimum node size fixed at 5.

Gradient boosted regression modeling (GBM) was implemented via *gbm* with fixed structural settings (shrinkage = 0.01, max interaction depth = 3, min observations per node = 10); the number of boosting trees (*n.trees*, up to 3,000) was selected by 5-fold internal cross-validation minimizing multinomial log-loss. EXtreme gradient boosting (XGBoost) was implemented via *xgboost* with fixed settings (max tree depth = 3, learning rate $\eta = 0.1$, row subsampling = 0.9, column subsampling = 0.8); the number of boosting rounds (*nrounds*, up to 500) was determined by 5-fold cross-

validation with early stopping after 20 consecutive rounds without improvement in multinomial log-loss.

Shrinkage discriminant analysis (SDA; *sda* package), regularized discriminant analysis (RDA; *klaR* package), generalized linear model boosting (glmBoost; *mboost* package), partial least squares regression for generalized linear models (plsRglm; *plsRglm* package), and classification and regression trees (CART; *rpart* package) were all trained within the *caret* framework with 5-fold cross-validation and tuneLength = 5, yielding five-point candidate grids for each algorithm's native parameters: shrinkage intensity λ and diagonal regularization δ for SDA; covariance shrinkage λ and scaling γ for RDA; boosting iterations mstop and prune for glmBoost; number of latent components nt for plsRglm; and complexity parameter cp for CART. The configuration yielding the highest mean cross-validated AUC was selected for final model fitting. A complete summary of all hyperparameter configurations is provided in Supplementary Table S10.

References

1. Luo L, Dong F, Li D, Li X, Li X, Fan Y, Qi C, Luo J, Li L, Shen B. Enhancing 3D DNA Walker-Induced CRISPR/Cas12a Technology for Highly Sensitive Detection of ExomicroRNA Associated with Osteoporosis. ACS Sens. 2024, **9:**1438-1446.
2. Shen B, Li L, Liu C, Li X, Li X, Cheng X, Wu H, Yang T, Cheng W, Ding S. Mesoporous Nanozyme-Enhanced DNA Tetrahedron Electrochemiluminescent Biosensor with Three-Dimensional Walking Nanomotor-Mediated CRISPR/Cas12a for Ultrasensitive Detection of Exosomal microRNA. Anal. Chem. 2023, **95:**4486-4495.
3. Xie Z, Zhao S, Deng R, Tang X, Feng L, Xie S, Pi Y, Chen M, Chang K. Logic-Measurer: A Multienzyme-Assisted Ultrasensitive Circuit for Logical Detection of Exosomal MicroRNAs. ACS Nano. 2025, **19:**12222-12236.
4. Wang YZ, Li YR, Zhang YQ, Xiang YM, Bai RR, Liu Y, Li ML, Meng GR, Pan SL, Zhang F, et al. Dual-signal ratiometric electrochemiluminescence biosensor based on Au NPs-induced low-potential emission of PFO Pdots and LSPR-ECL mechanism for ultra-sensitive detection of microRNA-141. Biosens. Bioelectron. 2024, **261:**116495.
5. Xie W, Jia S, Yu R, Xue J, Bai S, Wang C, Tian G, Zhang Q, Gui X, Wang L, et al. Portable miRNA profiling of sepsis-associated exosomes via a novel DNA molecular lock-mediated nanobiosensor. Chem. Eng. J. 2025, **520:**166485.
6. Shen B, Wu Q, Fan Y, Wu H, Li X, Zhao X, Wang Y, Ding S, Zhang J. TiO_2@Ag nanozyme enhanced electrochemiluminescent biosensor coupled with DNA nanoframework-carried emitters and enzyme-assisted target recycling amplification for ultrasensitive detection of microRNA. Chem. Eng. J. 2022, **445:**136820.
7. Sun Y, Fang L, Han Y, Feng A, Liu S, Zhang K, Xu JJ. Reversible Ratiometric Electrochemiluminescence Biosensor Based on DNAzyme Regulated Resonance Energy Transfer for Myocardial miRNA Detection. Anal. Chem. 2022, **94:**7035-7040.